Computer animation as a tool to visualize effects of seismic wave propagation inside heterogeneous media

Arrigo Caserta ([1]) **and Piero Lanucara** ([2])
([1]) *Istituto Nazionale di Geofisica, Roma, Italy*
([2]) *C.A.S.P.U.R., Università «La Sapienza», Roma, Italy*

Abstract
A technique to make computer animations representing the propagation of antiplane shear waves in heterogeneous dissipative media is presented. The aim is to develop a useful tool to better investigate the physics of site effects in the 2D approximation. We apply this technique to real case studies that were the subject of previous papers. For each case study a movie has been made to illustrate the wavefield time evolution and its interaction with the geological structure. All the movies can be seen and downloaded at the web site http://sigfrido.ingrm.it/movies.html. The paper shows the most representative frames of movies, providing an overview of the role played by the topographic irregularities and the geometry of internal discontinuities in trapping and focusing energy. The details of the dynamics are well visualized through movies. Particular attention is devoted to the representation of simulated ground motion in sediment-filled basins under resonance conditions. Problems related to color scales and frame normalization are analysed and discussed.

Key words *computer animations – numerical modelling – seismic wave propagation*

1. Introduction

Numerical modelling is a powerful approach to investigate the physics of site effects (Bard and Bouchon, 1980a,b; Sánchez-Sesma, 1987, 1990; Paolucci *et al.*, 1992; Bard, 1995, 1999) as well as to estimate parameters commonly used for earthquake engineering purposes (Fäh *et al.*, 1993; Rovelli *et al.*, 1994, 1995a,b). This is particularly true for urban areas where the instrumental approach may not always be used because of the high level of cultural noise. Numerical simulations are largely applied mainly in 2D models, and many computer codes are available today (Moczo, 1989; Sánchez-Sesma and Campillo, 1991; Zahradnik *et al.*, 1993; Padovani *et al.*, 1995; Zahradnik and Priolo, 1995; Zahradnik and Moczo, 1996). These codes are usually employed to generate synthetic seismograms along the free surface of the model. To gain further insight into the role played by velocity discontinuities in reflecting and transmitting energy, snapshots of seismic wave amplitude inside the medium are also used (Kawase, 1996; Pitarka *et al.*, 1998).

This paper is aimed to introduce another useful tool in investigating the details of seismic wave propagation in nearsurface heterogeneous layers: computer animation. Nowadays powerful workstations allow us to set up a huge number of snapshot sequences that can be used to make movies with a great resolution in time. The aim is to associate the details of synthetic seismogram waveforms to the dynamical behaviour of the nearsurface geological structure. In other words, a sequence of frames allows us to follow

Mailing address: Dr. Arrigo Caserta, Istituto Nazionale di Geofisica, Via di Vigna Murata 605, 00143 Roma; e-mail: caserta@sigfrido.ingrm.it

the evolution in time of the wavefield inside heterogeneous media. Computer animations are particularly suited to identifying the occurence of wave interference that is often responsible for local amplitude variations with important implications for seismic hazard.

Ad hoc numerical experiments will be discussed. These experiments are selected as representative of two different situations:

– A large valley characterized by vertical wave reverberations and generation of surface waves from the edges.

– A narrow valley where the horizontal and the vertical size of the soft infilling are comparable, thus causing 2D resonances.

The effects produced by an incidence angle variation are also discussed in the example of the narrow valley.

2. The method

To generate the sequence of the movie frames we adopted the 2D modelling technique proposed by Caserta (1998). We briefly recall here the main guidelines of this method. It is based on the formulation of an initial boundary value problem which represents the viscoelastic dynamics driving out-of-plane wave propagation. The medium is dissipative with arbitrary 2D shape and topography. The discretization scheme, based on a finite-difference technique, is developed to study the response of the medium under the action of a forcing term simulating a plane wave with vertical or oblique incidence. The oblique incidence is solved by rotating the 2D model. To account for absorption, the rheological model of the generalized Maxwell body of Emmerich and Korn (1987) was chosen because of its superiority both in accuracy and in computational efficiency. Its formulation for heterogeneous media was generalized to include the stress-free boundary conditions (Caserta, 1998). Computations were made in the time domain. The results are synthetic seismograms on the free surface and snapshots of the wave amplitude inside the 2D profile (for further details see Caserta, 1998).

We present now a technique to use these snapshots to make computer animations. The sequence of frames has to be constructed to follow the evolution of waves propagating inside the medium. This is realized using a constant time-step between frames that has to be chosen according to wave velocity and size of layers.

The relationship between colorscale and numerical values of the wavefield is made by defining a law of the type

$$y = F(x)$$

which links the numerical values (x) to colors (y) of a chosen colorscale. $F(x)$ is here called the Association Function (AF).

Let first consider a crude normalization obtained by dividing the instantaneous amplitude by the maximum value through all the frames. If the absolute value of the wave amplitude is considered, and a standard colorscale is used, the plot of AF is a straight line (V in fig. 1). But such a linear relation between numerical values and colors is not necessarily the optimal one to emphasize all the details of the internal dynamics. Other mathematical relations between normalized numerical values and colors could be more appropriate. One of the easiest alternative expressions is a branch of parabol. Its equation is

$$y = ax^2 + bx + c. \qquad (2.1)$$

The numerical values of the parameters a, b and c must be chosen to obtain a more convenient AF which better represents the details of the dynamics. We have three parabol coefficients so we need three constraints:

1) The point (0,0) in the (x, y) plane belongs to the parabol.

2) y must be equal to 1 when $x = 1$.

3) To avoid the case where different numerical values are represented with the same color, we require that the x coordinate of the parabol vertex must be ≥ 1.

Summarizing:

$$\begin{cases} c = 0 \\ |a| + b = 1 \\ -\dfrac{b}{2|a|} \geq 1. \end{cases} \qquad (2.2)$$

If we want an *amplification color* effect our parabol must have its concavity downward. From (2.2) it follows:

$$\begin{cases} c = 0 \\ a + b = 1 \\ -1 \le a \le 0 . \end{cases} \tag{2.3}$$

On the basis of eqs. (2.3), we can choose the numerical value of a within the range -1 to 0 including the two extremes. When a tends to zero the parabol tends to the straight line V of fig. 1. Other curves are shown in fig. 1 for a different choice of the parabol parameters.

3. Applications

All the applications considered in this paper deal with the out-of-plane dynamical behaviour

	a	b	c
I	-1.3	2.3	0.0
II	-1.0	2.0	0.0
III	-0.7	1.7	0.0
IV	-1/2	3/2	0.0
V	0.0	1.0	0.0

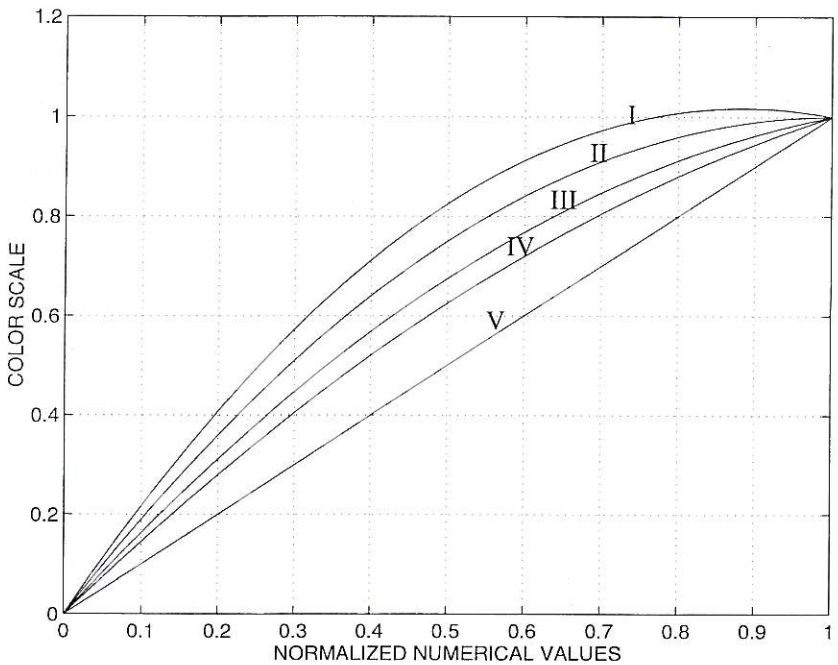

Fig. 1. Behaviour of function (2.1) for different values of parameters a, b, c.

of 2D sedimentary valleys excited by a vertically or obliquely incident plane wave. The first basin (the Tiber river valley in Rome) is chosen as representative of a situation where width (2000 m, approximately) is significantly greater than depth (60 m). As shown by Bard and Bouchon (1985), such basins are characterized by 1D resonance and horizontal propagation of surface waves generated at the basin edges. The Tiber river valley is the main sedimentary body of the city and has been extensively studied by several authors (Fäh *et al.*, 1993, 1995; Boschi *et al.*, 1994; Rovelli *et al.*, 1994; Rovelli *et al.*, 1995a,b; Tertulliani and Riguzzi, 1995; Cifelli *et al.*, 1999; Caserta *et al.*, 1999).

The other valley used for movie applications is characterized by a width comparable with depth (both of the order of a hundred metres). For such basins the 2D resonance is expected to occur. As an example, the geological structure underlying the Roman Colosseum first studied by Moczo *et al.* (1995) is here modelled for both delta-like and monochromatic incident plane waves. The same valley will also be used for the last application where the differences between vertical and oblique incidence are also discussed.

The paper will show only a few frames representing the wavefield amplitude at different times. The whole wavefield evolution in time for all the case studies can be found at the web site http://sigfrido.ingrm.it/movies.html; each movie at the web site can be seen and downloaded.

3.1. *The Tiber valley*

Figure 2 shows a 2D digitized vertical profile of the Tiber valley representing the historical centre of Rome as modelled by Boschi *et al.* (1994). On the top of fig. 2 elastic and anelastic parameters used in our numerical modelling are listed. Synthetic seismograms representing antiplane horizontal ground motion on the free surface are shown as well. These numerical simulations have been made using a grid-step of 1.56 m and a time-step of 0.0018 s, that guarantee accuracy of the finite-difference technique up to 8 Hz. Seismic input is a vertically incident plane wave realized starting from a Gabor impulse as described in Caserta (1998)

$$g(t) = \exp\left[-\left(\frac{\omega_p (t - t_s)}{\gamma}\right)^2\right] \cos[\omega_p (t - t_s) + \psi] \tag{3.1}$$

where $\omega_p = 2\pi f_p$, $t_s = 0.45\gamma/f_p$. f_p is the predominant frequency of the impulse.

Synthetic seismograms of fig. 2 show that, in the valley, energy goes back and forth between the free surface and the bottom of the soft layer. This behaviour is the so-called 1D resonance. At the same time a horizontal propagation of locally generated surface waves occurs inside the basin starting from the valley edges. This dynamic behaviour of large valleyes was first discussed by Bard and Bouchon (1985) who demonstrated that the transition from 1D resonance plus lateral propagation to 2D resonance is a function of the impedance contrast and the ratio between width and depth.

In fig. 2 the effects of diffraction are also evident on the two hills delimitating the valley. On the right side, a single diffracted wavetrain is travelling inside the volcanic deposits, starting from the right edge and propagating toward the right-hand side. On the contrary, much more complex wavetrains start from the left edge toward the left-hand side of the profile. This difference between the two edges is probably due to the highly irregular topography and the more complex geometry of the hidden discontinuities under the left basin edge.

Figure 3 shows a sequence of snapshots representing the amplitude of displacement for different time values. The entire movie is presented at the web site http://sigfrido.ingrm.it/movies.html. The role played by the hidden discontinuities is well described by the sequence of snapshots (fig. 3) that helps clarify the details of synthetic seismograms. Energy is trapped in the basin producing vertical reverberations (see frames from $T = 0.58$ s to $T = 1.06$ s); at the same time, surface waves are generated by the valley edges. The yellow spots, horizontally propagating below the surface in the basin from frame $T = 0.80$ s, well visualize this effect. The higher complexity of nearsurface geology at the left basin edge is also responsible for a lower effi-

Geological Units	P-wave velocity (m/s)	S-wave velocity (m/s)	Density (g/cm^3)	Quality Factor
1: Manmade Fill	250	150	1.95	5
2: Holocene Alluvium	450	300	1.95	10
3: Volcanic Deposits and Pleistocene Sediments	600	400	2.0	20
4: Pliocene Bedrock	1200	600	2.1	50

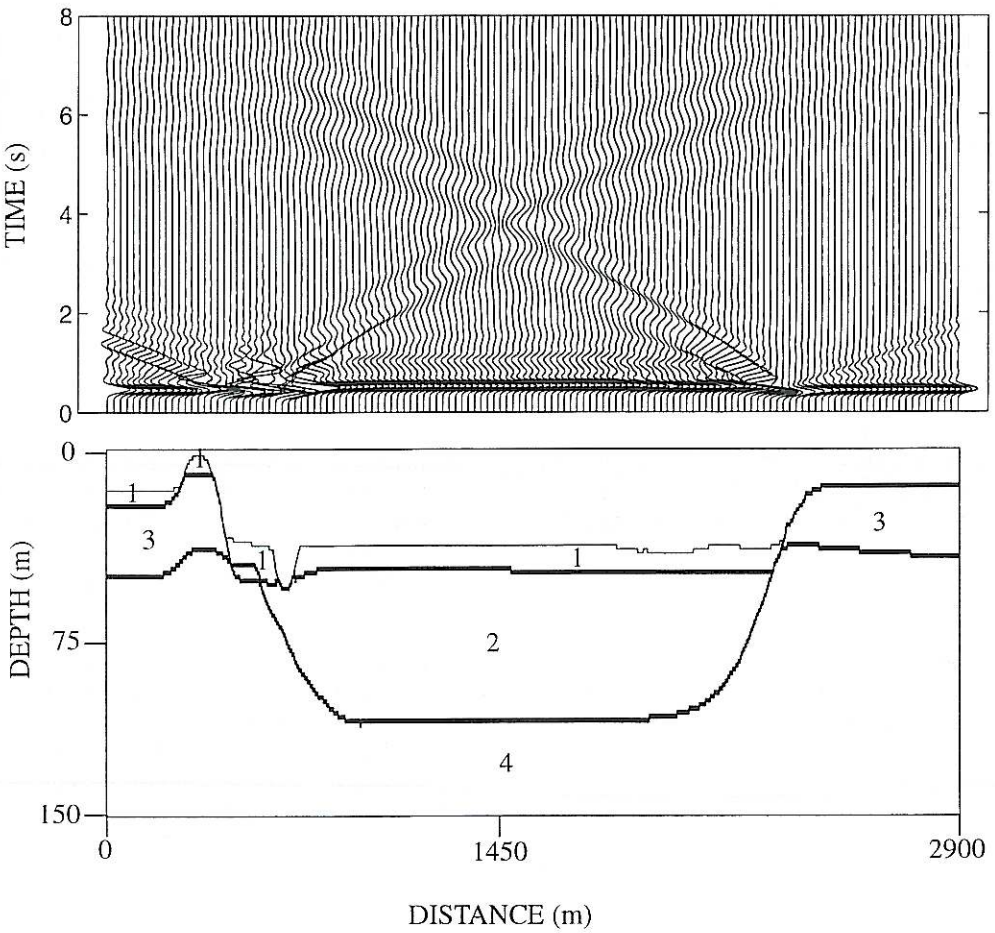

Fig. 2. Delta-like transient response of a 2D section of the Tiber valley in Rome, for a vertically incident plane wave.

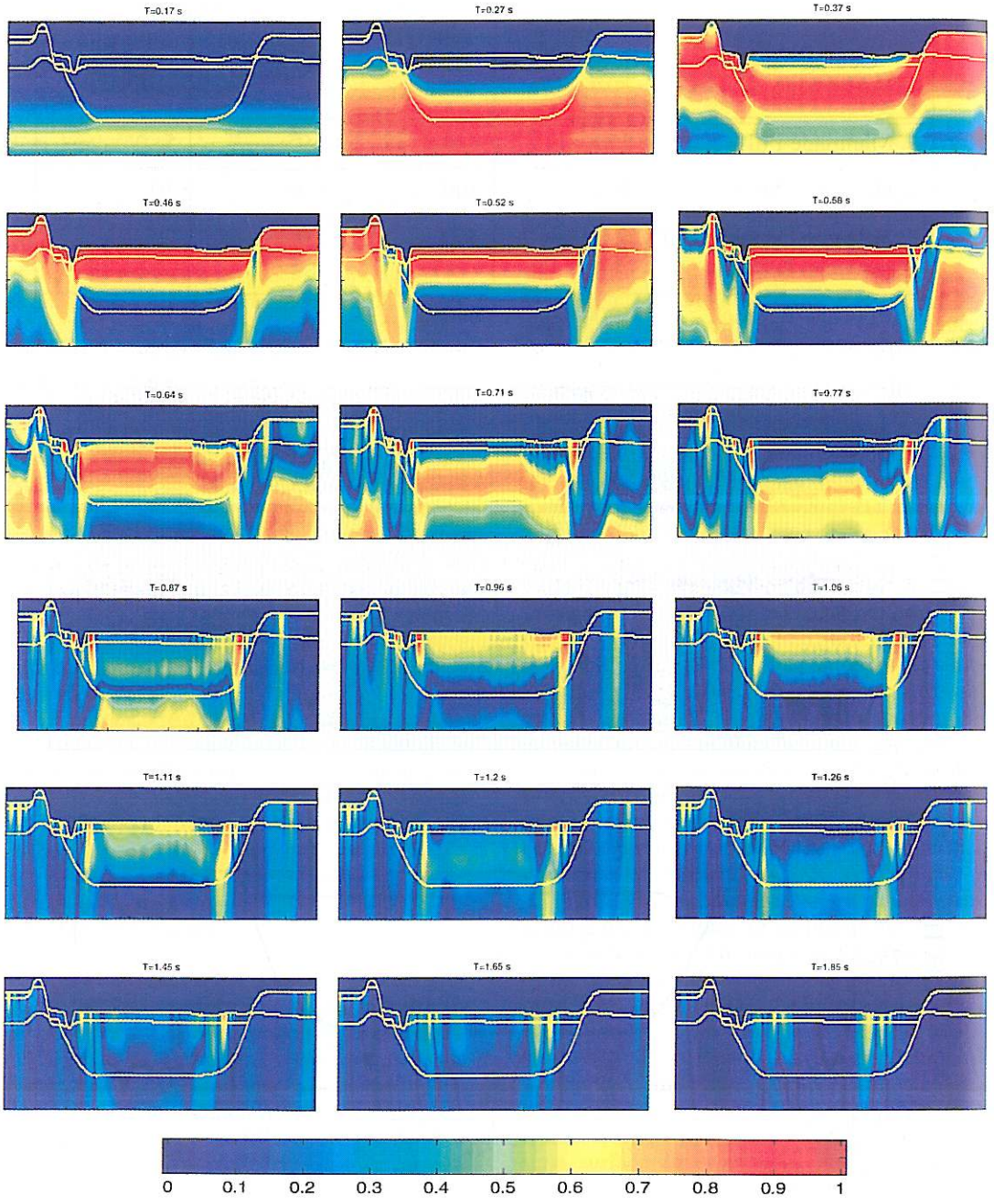

Fig. 3. Sequence of snapshots representing wave amplitude inside the 2D model of the Tiber valley. The chosen AF is curve I of fig. 1.

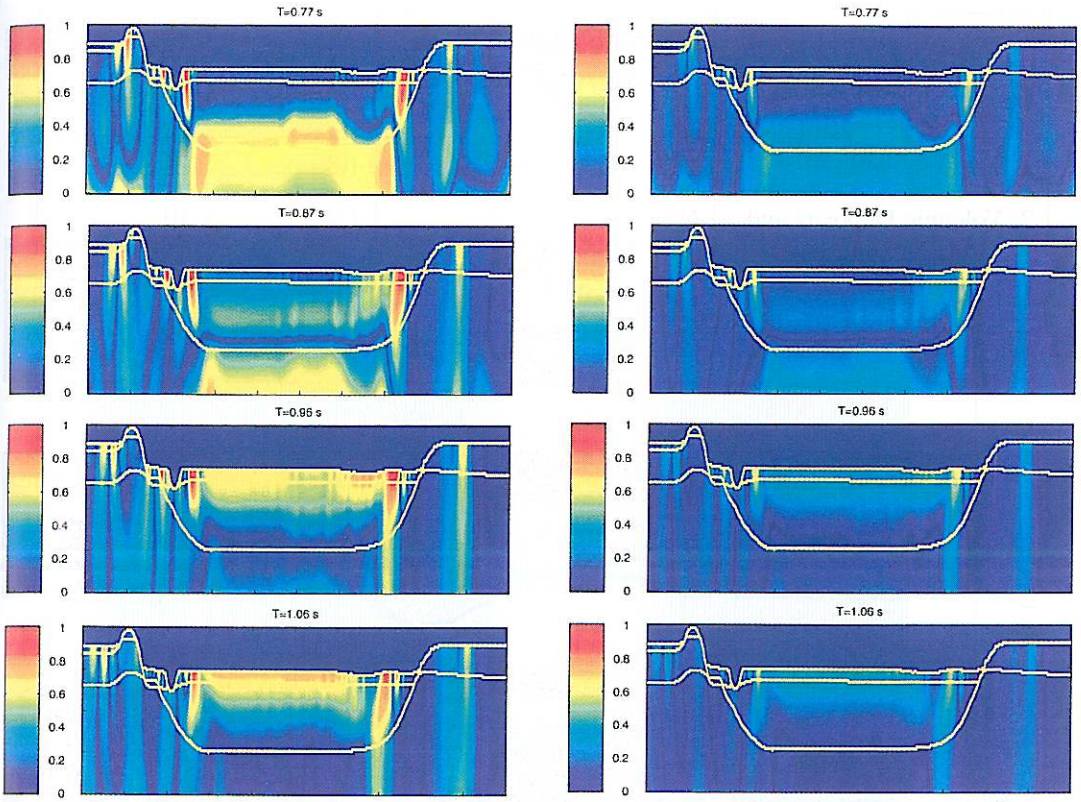

Fig. 4. Comparison between snapshots obtained using different AF curves for frames including the vertical reverberation (curve I on the left and curve V on the right).

ciency in generating surface wavetrains compared to the right edge (this is evident in frames from $T = 0.77$ s to $T = 1.11$ s).

Frames in fig. 3 are realized using an AF corresponding to curve I in fig. 1. This means that, compared to the 1:1 relation (curve V), colors are saturated in the amplitude range 0.73 to 1. Saturation is intentionally introduced to better visualize the dynamical behaviour after the wave front is rebounded from the free surface. If we use curve V of fig. 1, we obtain the result shown in the right column of fig. 4. The comparison between frames obtained using different AFs reveals the importance of an appropriate choice for the association function (see fig. 4) in order to properly point out the most important physical features of wave propagation.

3.2. *The Colosseum valley*

The second case study is a valley whose horizontal and vertical dimensions are comparable. Figure 5 shows the synthetic seismograms obtained for the antiplane horizontal motion along the free-surface of this valley. The geological structure belongs to the site where the Roman Colosseum was built. Values of elastic and anelastic parameters used for the numerical modelling are also shown in fig. 5. The geological structure and seismic response of this small valley were first studied by Funiciello *et al.* (1995) and Moczo *et al.* (1995). The total cross-sectional area is 982 m long and 117 m deep; values of 0.5 m and 0.00039 s are used in the numerical modelling for the grid-step and time-

Geological Units	P-wave velocity (m/s)	S-wave velocity (m/s)	Density (g/cm)	Quality Factor
1:Holocene Alluvium	180	100	1.8	15
2: Volcanic Deposits and Pleistocene Sediments	600	400	1.9	40
3: Pliocene Bedrock	1600	800	2.05	100

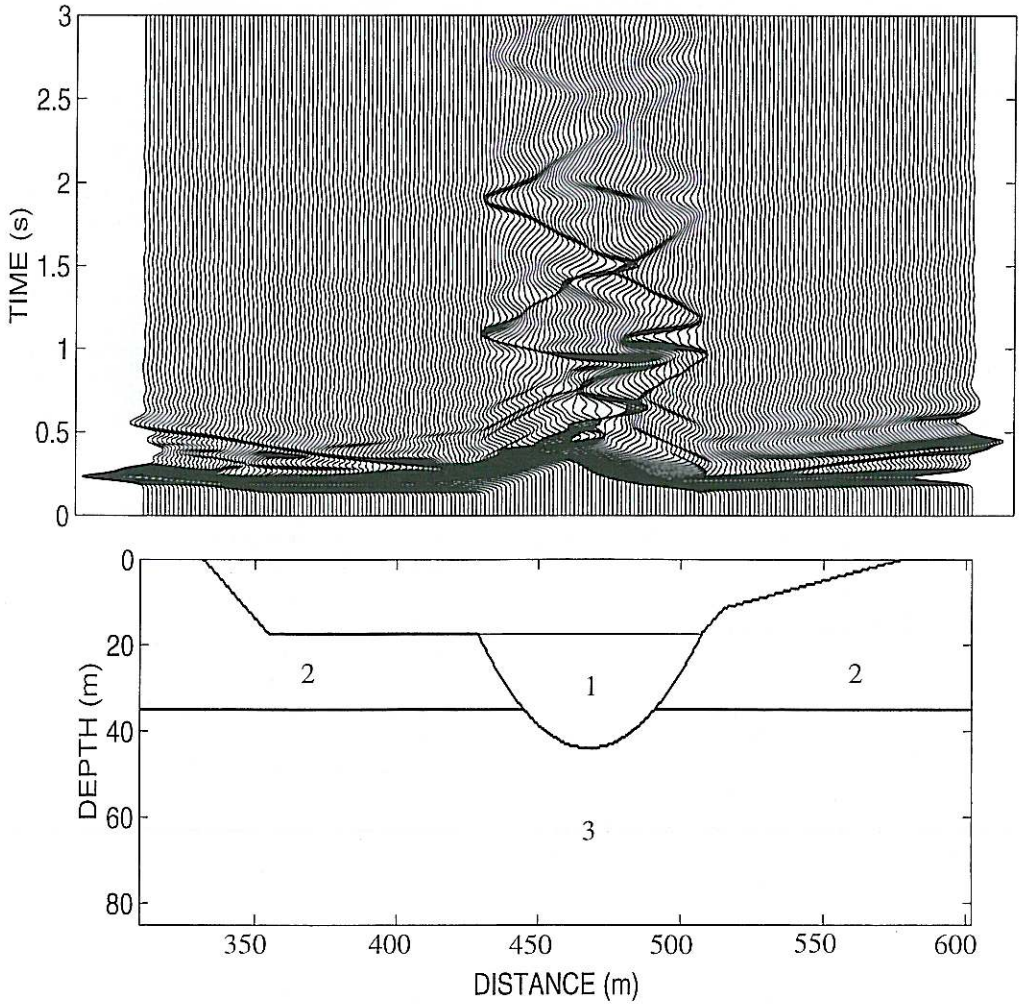

Fig. 5. Delta-like transient response of a 2D model of the Colosseum valley for a vertically incident plane wave.

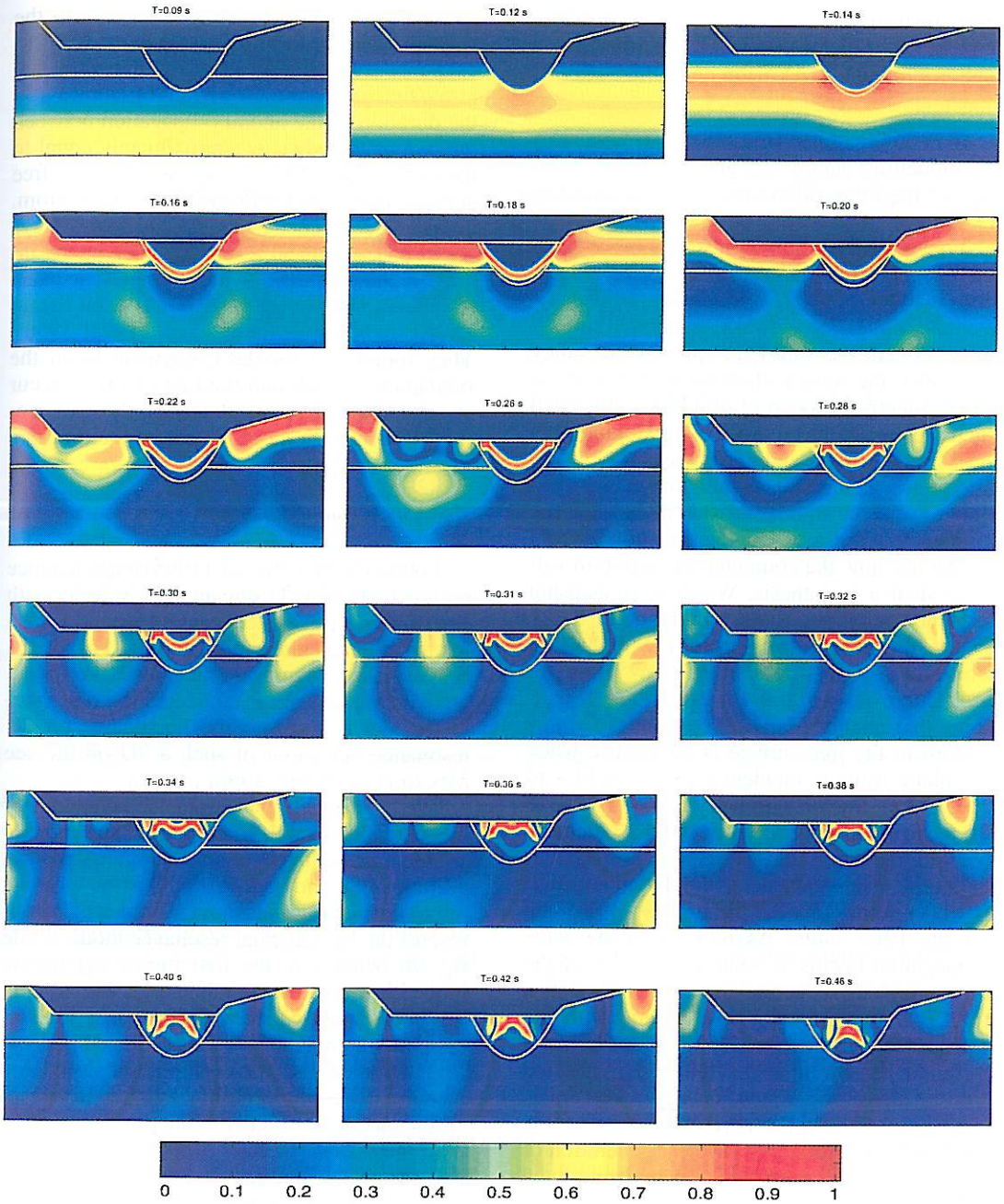

Fig. 6. Sequence of snapshots representing wave amplitude inside the 2D model of the Colosseum valley for a vertically incident plane wave.

step, respectively. The incident radiation is a plane wave delta-like input described by a Gabor function (3.1) with the following parameters: $\gamma = 0.08$, $f_p = 0.45$, $\psi = \frac{\pi}{2}$ and $t_s = 0.07410$ (see Caserta, 1998). This choice of the modelling parameters guarantees the accuracy of the finite-difference computation up to 15 Hz.

Looking at the synthetic seismograms of fig. 5, we recognize both the vertical energy reverberations in the central part of the valley and the horizontal propagation of locally generated surface waves within the valley. In spite of the valley symmetry, the wave pattern inside the valley is not symmetric. Moczo *et al.* (1995) attributed such a feature to the presence of the sloping free-surface at the right-hand side of the basin. In their interpretation, this slope would favour energy to flow toward the right-hand side decreasing the efficiency of diffraction at the right edge.

We use now the computer animation to validate such a hypothesis. We draw a snapshot sequence belonging to the simulation of fig. 5. Figure 6 shows frames from $T = 0.09$ s to $T = 0.46$ s. In this case, after a few trials, we used curve II of fig. 1 for AF. These frames show that energy propagating from the valley bottom to the free-surface is symmetric when the plane wave is incident (see $T = 0.14$ s to $T = 0.22$ s). Such a symmetry is mainly due to the basin dimensions, *i.e.*, the width is comparable with the depth; in this case the propagation of energy inside the basin is fully symmetric. It is worth noting that the same does not happen for the Tiber valley. Asymmetry in the wave propagation begins as soon as the roles of the diffracting edges become important ($T = 0.28$ s to $T = 0.34$ s). Energy reverberations in the subsurface layers external to the basin follow a different behaviour at the left and right-hand sides. Out of the valley, energy reverberates vertically in the upper horizontal layer on the left-hand side producing efficient generation of surface waves in the basin. On the right-hand side the presence of the slope decreases the conversion toward the valley interior. Frames from $T = 0.32$ s to $T = 0.42$ s show that energy is flowing outward as surface wave-trains propagating along the slope. The computer animation provides clear visual evidence that confirms the validity of inferences by Moczo *et al.* (1995).

The computer animation at the web site http://sigfrido.ingrm.it/movies.html shows that the duration of the lateral propagation between the two valley edges is approximately equal to the time required by energy to reach the free surface after being reflected from the bottom. This feature cannot occur for shallow valleys and produces typical resonance phenomena involving the whole sedimentary basin. The basin response in resonance regime has been extensively studied by Moczo *et al.* (1995, 1996). They found that for the Colosseum basin the fundamental mode and the first overtone occur at 1.2 and 2.4 Hz, respectively. In the next section we deal with these 2D resonance modes.

3.3. *The resonance regime*

Following Moczo *et al.* (1995) the resonance regime is simulated using an input wavelet with a narrow spectral content centred around 1.2 Hz for the fundamental mode, and 2.4 Hz for the first overtone. Figures 7 and 8 show the fundamental antiplane shear mode and the first symmetric mode, respectively. For details on the resonance behaviour of such a 2D profile see Moczo *et al.* (1995, 1996).

We look now at the resonance behaviour of the whole 2D model, and not only the synthetic seismograms on the free surface. Figure 9a shows a frame of the movie *Reso1.mpg* at the web site http://sigfrido.ingrm.it/movies.html which represents the fundamental resonance mode, while fig. 9b belongs to the first higher symmetric mode illustrated through the movie *Reso2.mpg*. To better visualize the resonance modes, in these computer animations we have changed the representation of the wave amplitude inside the medium. The whole basin oscillates in a synchroneous way normally to the profile. The displacement field changes smoothly and coherently from the minima to the maxima with a regular evolution in time. Therefore displacement colorscale is chosen symmetric around the zero value and normalized between -1 and 1. No magnification of the normalized numerical values is needed, and curve V of fig. 1 is used.

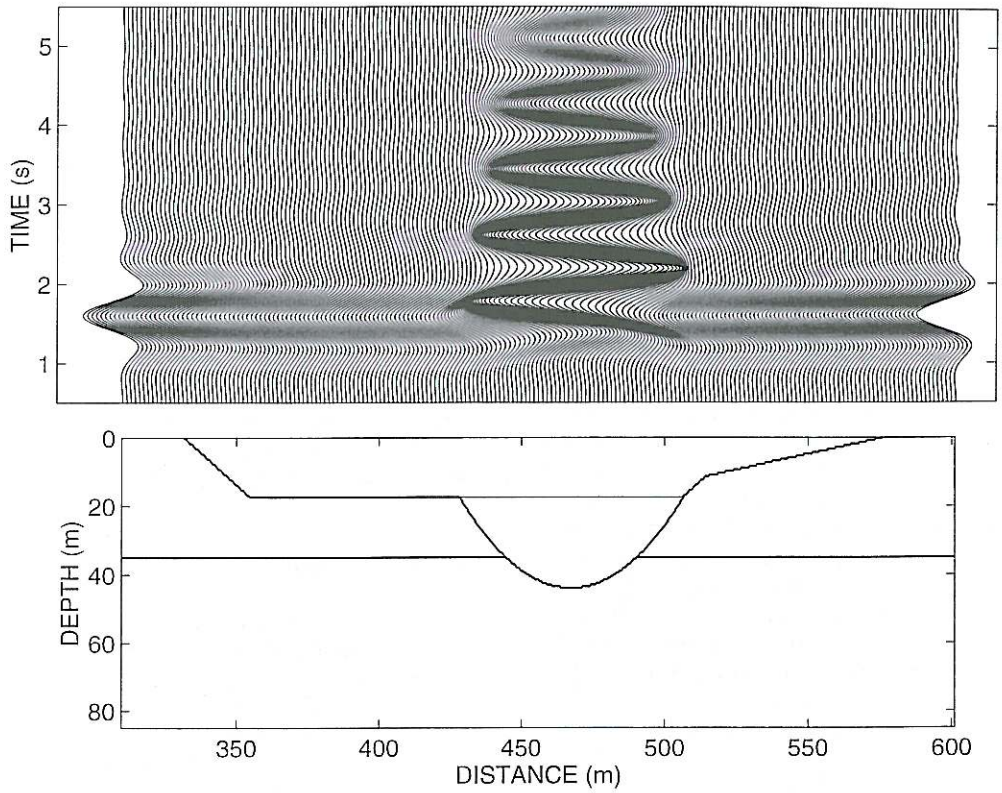

Fig. 7. Time-domain representation of the fundamental antiplane shear mode (1.2 Hz) of the 2D resonance of the Colosseum valley model.

3.4. *Oblique incidence*

As proposed by Caserta (1998), oblique incidence is simulated by rotating the model used for the vertical incidence. Synthetic seismograms generated by rotating the previous model of the Colosseum valley by an angle $\alpha = 30°$ are shown in fig. 6 of Caserta (1998). Such a rotation yields results that are equivalent to those obtained with an unrotated model for an obliquely incident plane wave coming from the right side. Material properties, grid and time steps are those used for the vertical incidence.

Figure 10 shows a sequence of frames generated using the model of fig. 5 for an oblique incidence of $\alpha = 30°$. These frames belong to the movie *Colobli.mpg* at the web site http://sigfrido.ingrm.it/movies.html. The association function between color-scale and normalized numerical values is the same as that used in the vertical incidence (curve II in fig. 1). Many differences emerge with respect to the vertical incidence. The main one is that wavetrains diffracted toward the left-hand side have higher energy than those diffracted toward the right-hand side. This is due to the higher diffraction efficiency of the side facing the incoming wavefront. The second important difference is asymmetry in trapping energy in the upper layer out of the valley. While the energy flows out of the model on the left-hand side, at the right-hand side energy reverberations in the volcanic layer reinforce the generation of surface waves in the basin.

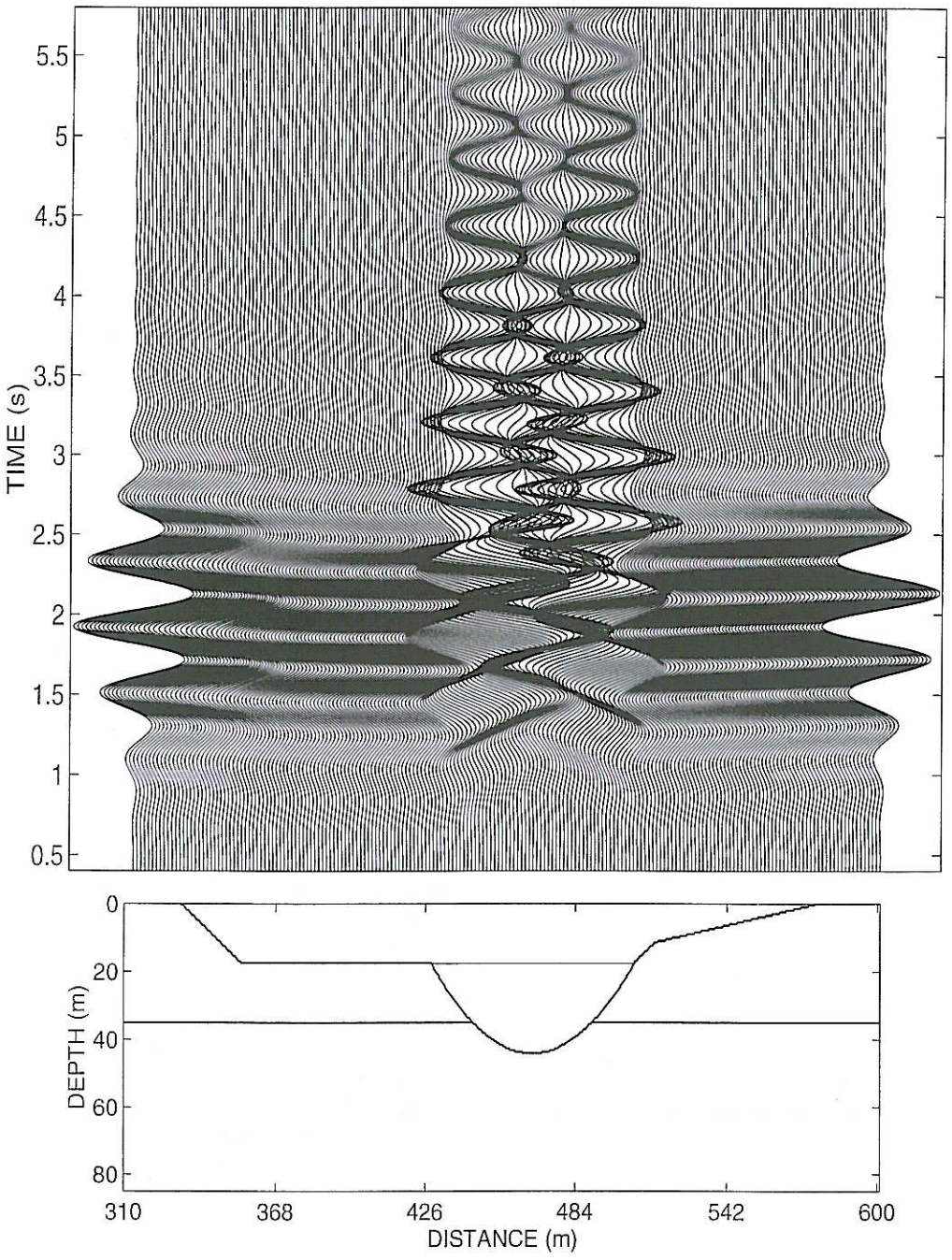

Fig. 8. Time-domain representation of the first higher symmetric shear mode (2.4 Hz) of the 2D resonance of the Colosseum valley model.

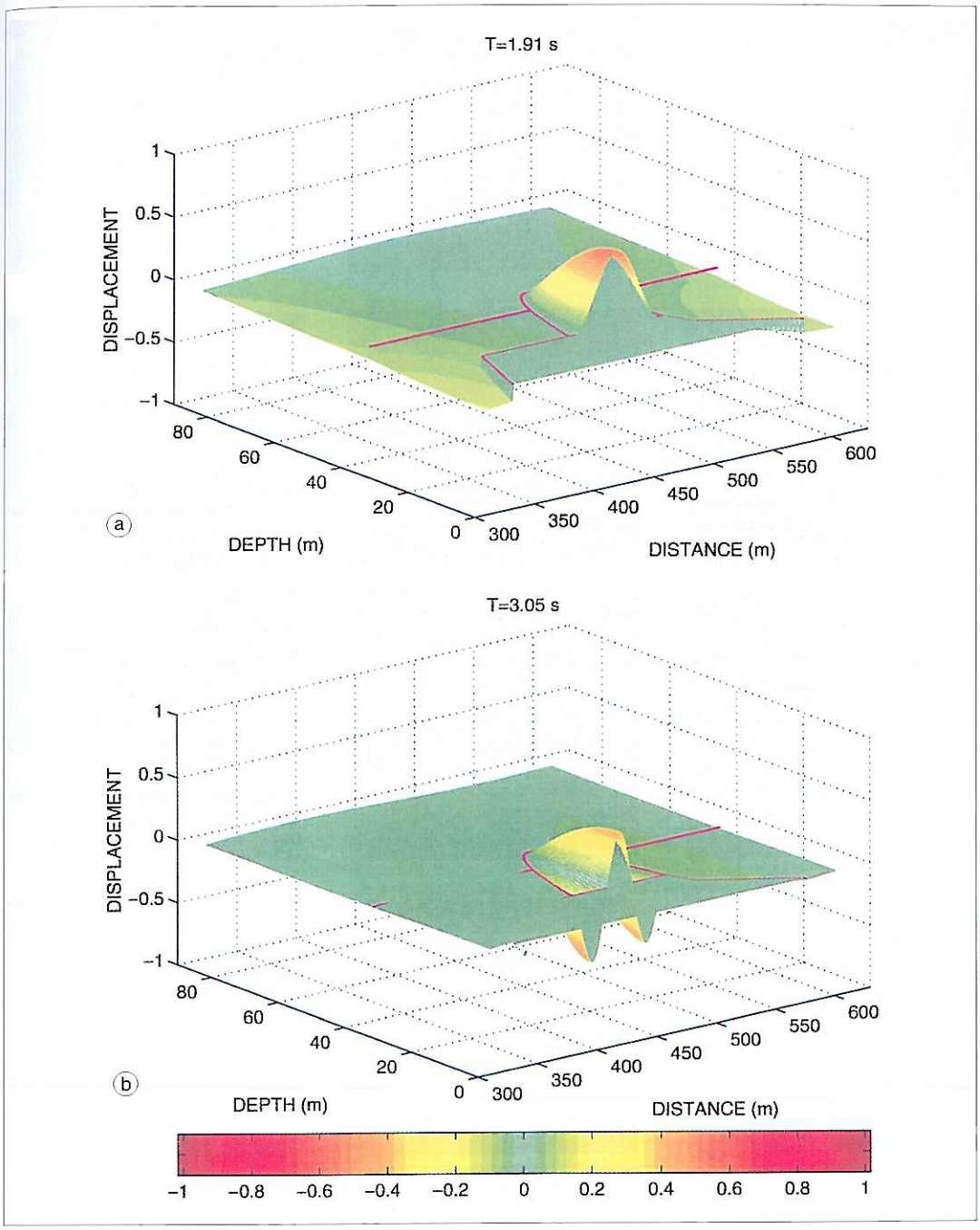

Fig. 9a,b. Representative frames of movies belonging to the fundamental mode (a), and to the first overtone, (b) (from movies *Reso1.mpg* and *Reso2.mpg*, respectively).

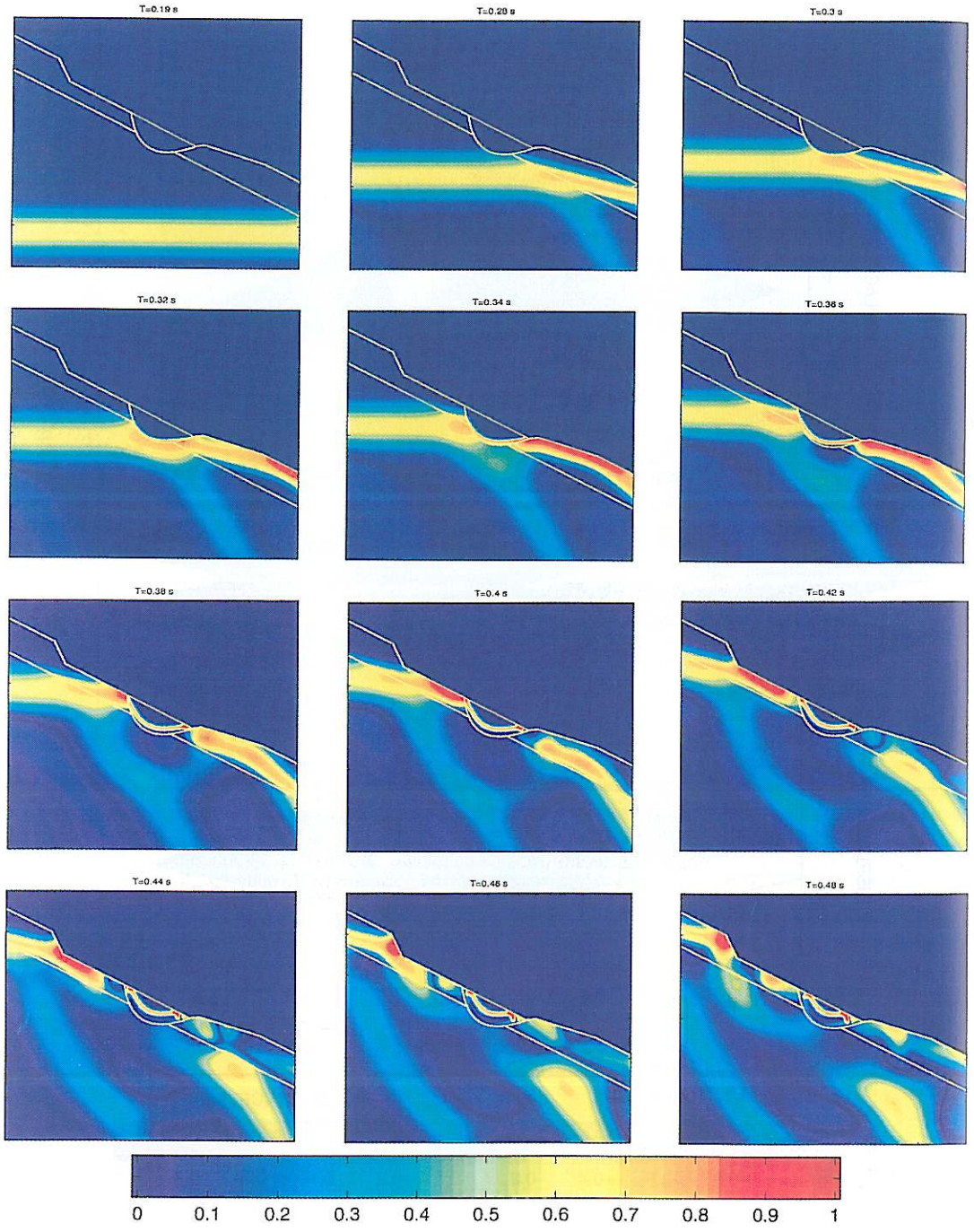

Fig. 10. Sequence of snapshots representing wave amplitude inside the 2D model of the Colosseum valley for a obliquely incident plane wave. Angle of incidence is 30°.

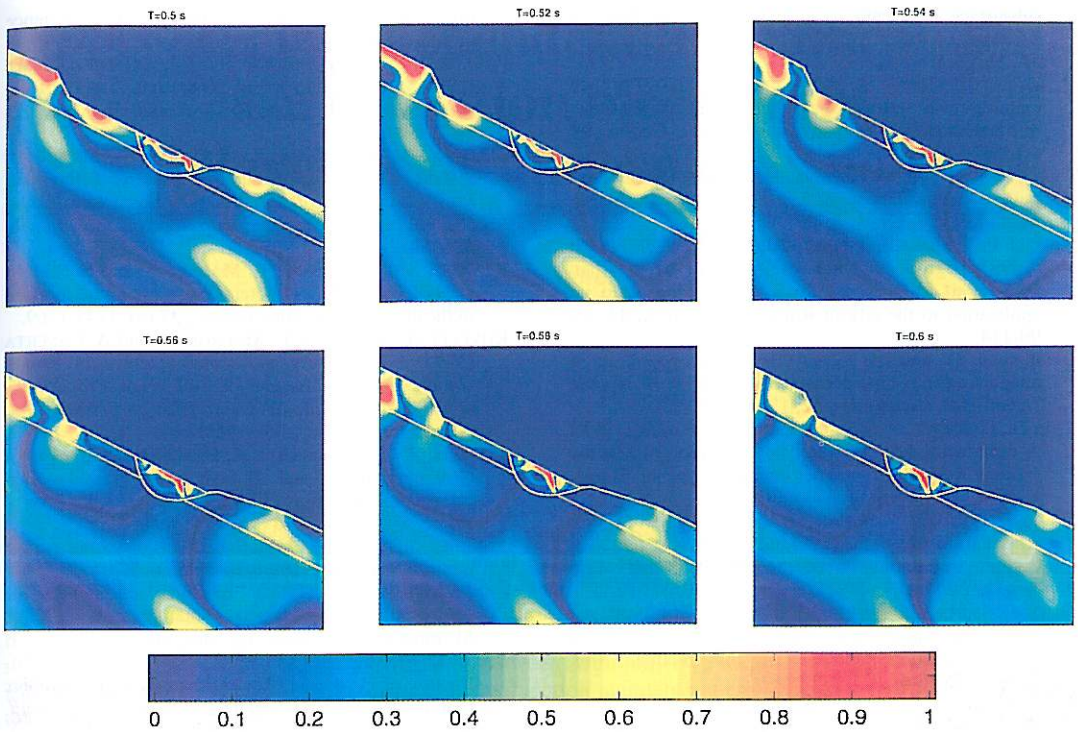

Fig. 10 (*continued*).

4. Conclusions

We have presented a technique to make movies from sequences of snapshots generated by computer simulations. We applied this technique to antiplane waves in the 2D approximation using the numerical code of Caserta (1998). It has been shown that the choice of an appropriate relation between amplitude normalization and colorscale is crucial to enhance the most important features of the dynamical behaviour of complex geological structures. A general rule for such a choice does not exist, nevertheless from numerical experiments some hints arise.

We tested one of the easiest non-linear association relations between normalized numerical values and colors, *i.e.* the parabolic one. In spite of its simplicity, the results suggest that after a few attempts the dynamical behaviour of complex geological structures can be satisfactorily visualized by the snapshot sequence.

REFERENCES

BARD, P.-Y. (1995): Effects of surface geology on ground motion: recent results and remaining issues, in *Proceedings of the 10th European Conference on Earthquake Engineering, 28 August - 3 September 1994*, Vienna, Austria (Gerald Duma Editor), **2**, 305-324.

BARD, P.-Y. (1999): Microtremor measurements: a tool for site effects estimation?, in *Proceedings of the Second International Symposium on the Effects of Surface Geology on Seismic Motion, 1-3 December 1998* (A.A. Balkema Editor, Rotterdam, Netherlands), 1251-1279.

BARD, P.-Y. and M. BOUCHON (1980a): The seismic response of sediment-filled valleys. Part 1. The case of incident *SH* waves, *Bull. Seismol. Soc. Am.*, **70**, 1263-1286.

BARD, P.-Y. and M. BOUCHON (1980b): The seismic response of sediment-filled valleys. Part 2. The case of incident *P* and *SV* waves, *Bull. Seismol. Soc. Am.*, **70**, 1921-1941.

BARD, P. and M. BOUCHON (1985): The two-dimensional resonance of sediment-filled valleys, *Bull. Seismol. Soc. Am.*, **75**, 519-541.

BOSCHI, E., A. CASERTA, C. CONTI, M. DI BONA, R. FUNICIELLO, L. MALAGNINI, F. MARRA, G. MARTINES, A. ROVELLI and S. SALVI (1994): Resonance of

subsurface sediments: an unforeseen complication for designers of roman columns, *Bull. Seismol. Soc. Am.*, **85**, 320-324.

CASERTA, A. (1998): A time domain finite-difference technique for oblique incidence of antiplane waves in heterogeneous dissipative media, *Ann. Geofis.*, **41** (4), 617-631.

CASERTA, A., J. ZAHRADNÍK and V. PLICKA (1999): Ground motion modelling with a stochastically perturbed excitation, *J. Seismol.*, **3**, 45-59.

CIFELLI, F., S. DONATI, F. FUNICIELLO and A. TERTULLIANI (1999): High-density macroseismic survey in urban areas. Part 1: proposal for a methodology and its application to the city of Rome, *Ann. Geofis.*, **42** (1), 99-114.

EMMERICH, H. and M. KORN (1987): Incorporation of attenuation into time-domain computations of seismic wave fields, *Geophysics*, **52**, 1252-1264.

FÄH, D., C. IODICE, P. SUHADOLC and G.F. PANZA (1993): A new method for the realistic estimation of seismic ground motion in megacities: the case of Rome, *Earthquake Spectra*, **4**, 643-668.

FÄH, D., C. IODICE, P. SUHADOLC and G.F. PANZA (1995): Application of numerical simulations for a tentative seismic microzonation of the city of Rome, *Ann. Geofis.*, **38** (5-6), 607-615.

FUNICIELLO, R., L. LOMBARDI, F. MARRA and M. PAROTTO (1995): Seismic damage and geological heterogeneity in Rome's Colosseum area: are they related?, *Ann. Geofis.*, **38** (5-6), 927-937.

KAWASE, H. (1996): The cause of the damage belt in Kobe: «The basin-edge effect», constructive interference of the direct *S*-wave with the basin-induced diffracted Rayleigh waves, *Seismol. Res. Lett.*, **67**, 25-34.

MOCZO, P. (1989): Finite-difference technique for *SH*-waves in 2D media using irregular grids - application to seismic response problem, *Geophysics*, **99**, 321-329.

MOCZO, P., A. ROVELLI, P. LABÁK and L. MALAGNINI (1995): Seismic response of the geologic structure underlying Roman Colosseum and a 2D resonance of a sediment valley, *Ann Geofis.*, **38** (5-6), 939-956.

MOCZO, P., P. LABÁK, J. KRISTEK and F. HRON (1996): Amplification and differential motion due to an antiplane 2D resonance in the sediment valleys embedded in a layer over the half-space, *Bull. Seismol. Soc. Am.*, **86**, 1434-1446.

PADOVANI, E., E. PRIOLO and G. SERIANI (1995): Low and high-order Finite Element Method (FEM): experience in seismic modeling, *J. Comp. Acoustic*, **28**, 845-885.

PAOLUCCI, R., M.M. SUAREZ and F.J. SÁNCHEZ-SESMA (1992): Fast computation of *SH* seismic response for a class of alluvial valleys, *Bull. Seismol. Soc. Am.*, **82**, 2075-2086.

PITARKA, A., K. IRIKURA, T. IWATA and H. SEKIGUCKI (1998): Three-dimensional simulation of the near fault ground motion for the 1995 Hyogoken Nanbu (Kobe), Japan, earthquake, *Bull. Seismol. Soc. Am.*, **88**, 428-440.

ROVELLI, A., A. CASERTA, L. MALAGNINI and F. MARRA (1994): Assessment of potential strong ground motions in the city of Rome, *Ann. Geofis.*, **37** (6), 1745-1769.

ROVELLI, A., D. MOLIN, L. MALAGNINI and A. CASERTA (1995a): Variability of damage pattern in Rome: combination of source and local effects, in *Proceedings of the 5th International Conference on Seismic Zonation, Nice, France*, 1359-1366.

ROVELLI, A., L. MALAGNINI, A. CASERTA and F. MARRA (1995b): Using 1D and 2D modelling of ground motion for seismic zonation criteria: results for the city of Rome, *Ann. Geofis.*, **38** (5-6), 591-605.

SÁNCHEZ-SESMA, F.J. (1987): Site effects on strong ground motion, *Soil Dyn. Earthquake Eng.*, **6**, 124-132.

SÁNCHEZ-SESMA, F.J. (1990): Elementary solutions for the response of a wadge-shaped medium to incident *SH* and *SV* waves, *Bull. Seismol. Soc. Am.*, **80**, 737-742.

SÁNCHEZ-SESMA, F.J. and M. CAMPILLO (1991): Diffraction of *P*, *SV*, and Rayleigh waves by topographic features: a boundary integral formulation, *Bull. Seismol. Soc. Am.*, **81**, 2234 - 2253.

TERTULLIANI, A. and F. RIGUZZI (1995): Earthquakes in Rome during the past one hundred years, *Ann. Geofis.*, **38** (5-6), 581-590.

ZAHRADNÍK, J. and P. MOCZO (1996): Hybrid seismic modelling based on discrete-wave number and finite-difference methods, *Pure Appl. Geophys.*, **158**, 21-38.

ZAHRADNÍK, J. and E. PRIOLO (1995): Heterogeneous formulation of elastodynamics equations and finite-difference schemes, *Geophys. J. Int.*, **120**, 663-676.

ZAHRADNÍK, J., P. MOCZO and F. HRON (1993): Testing four elastic finite-difference schemes for behaviour at discontinuities, *Bull. Seismol. Soc. Am.*, **83**, 107-129.

(received February 20, 1999;
accepted July 15, 1999)